Electric Gap Control in a Semiconductor

by M. C. SANTOS AND E. LORA DA SILVA

Department of Physics, University of Coimbra, Portugal
Department of Chemistry, University of Bath, UK

Abstract: We show that the Bi-Layer Graphene allows the control of its electronic gap under an applied voltage.

Keywords: Semiconductor, carbon allotropes.

1 Carbon Allotropes Double Layer Graphene

Many properties of single-layer graphene has been theoretically studied to allow further characterization of this material. These properties are unconventional due to the unique band structure of graphene, which is described in terms of Dirac fermions.

The experimental study of graphene triggered a growing attention to its electronic properties,[14] because the honeycomb lattice defines a band structure [19] with two nodal points in the Brillouin zone which determines a relativistic Dirac-type electronic dynamics [18] (creating links with certain theories of particle physics). These properties are responsible for unusual phenomena, such as the fractional Hall effect,[13, 20, 7, 16] which allows the possibility for magnetic catalysis of an excitonic gap,[6, 5, 10, 9, 8, 11] ferromagnetism and superconductivity. [12]

Other studies related to suspended graphene vacuum, revealed that graphene can change from a semi-metal into an insulator, due to the formation of a gap in the fermionic spectrum, resultant from the chiral symmetry breaking; condensate (exciton). [2, 1]

More recently, attention has turned to the multi-layer graphene [3] and, particularly, to the bi-layer graphene, which also reveals abnormalities, i.e., on the of Quantum Hall effect.[15] In fact, it was shown that the bi-layer graphene also shows unconventional behaviour in its properties, however, these properties are different from those observed in the single-layer of graphene.

There are two main reasons that explain the unconventional physics of multi-layered graphene:

1. The coupling between the layers is relatively weak and therefore some of the properties of the base material, the single layer of graphene, are manifested.

2. The peculiar geometry resulting from the A-B layer stacking (*Bernal stacking*), implies that the connection between the plans takes place mostly in one of the sub-lattices of each plan.

As in the case of the single-layer graphene, also the bi-layer graphene is sensitive to the inevitable disorder generated by environment of the SiO_2 substrate.

It has been theoretically and experimentally shown that the bi-layer graphene is the only material with semiconductor properties, with which the width of the electronic gap is proportional to an applied electric field.

2 Electric-Bias Control in Double Layer Graphene Electronic Gap

We will start start by describing the pure bi-layer graphene system with Bernal stacking, where we only consider the $t_\perp$ coupling amplitude between vertical layers restricted to shorter vertical distances of these carbon atoms. We apply between these planes the electric field f. The Fermi operators are represented in the second-quantization formalism as a Fourier transform of the n on-site operators $a_{\mathbf{n}}$

$$a_{\mathbf{k},j} = N^{-1/2} \sum_n e^{-\imath \mathbf{k}\cdot\mathbf{n}} a_{\mathbf{n},j} \tag{1}$$

which represent plane wave states with $\mathbf{k}$ moment, the indices j are related to four types of sites in the lattice and, N is the number of cells in a layer - see fig. 1. A $4-$spinor is formed as

$$a^\dagger_{\mathbf{k}} = \left(a^\dagger_{\mathbf{k},1}, a^\dagger_{\mathbf{k},2}, a^\dagger_{\mathbf{k},3}, a^\dagger_{\mathbf{k},4}\right) \tag{2}$$

and where the unperturbed Hamiltonian is presented as

$$H_0 = \sum_{\mathbf{k}} a^\dagger_{\mathbf{k}} \hat{H}_0 a_{\mathbf{k}} \tag{3}$$

with matrix

$$\hat{H}_0 = \begin{pmatrix} f & t_\perp & \gamma_{\mathbf{k}} & 0 \\ t_\perp & -f & 0 & \gamma^*_{\mathbf{k}} \\ \gamma^*_{\mathbf{k}} & 0 & f & 0 \\ 0 & \gamma_{\mathbf{k}} & 0 & -f \end{pmatrix} \tag{4}$$

where $\gamma_{\mathbf{k}} = t \sum_{\boldsymbol{\delta}} e^{\imath \mathbf{k}\cdot\boldsymbol{\delta}}$ is related to the in-plane hopping amplitude t, where the sum is performed over the vectors $\boldsymbol{\delta}$, connecting the nearest neighbours of the n sites.

In the Dirac points, $\mathbf{K} = (0, 4\pi/3\sqrt{3}a)$, and $-\mathbf{K}$, the function $\gamma_{\mathbf{k}}$ vanishes. This result occurs in the vicinity of $\mathbf{K}$: $\mathbf{q} = \mathbf{k} - \mathbf{K}$, is linear: $\gamma_{\mathbf{k}} \approx \hbar v_F(q_x - iq_y)$, where $v_F = 3ta/2\hbar$ (with v_F being the Fermi velocity, $v_F = c/300$, c the velocity of light in vacuum, and $\hbar$ the reduced Planck constant).

After diagonalizing the matrix, eq. 4, we obtain:

$$H_0 = \sum_{\mathbf{k}} \Big[\varepsilon_{\mathbf{k},1} \left(\alpha^{\dagger}_{\mathbf{k},1}\alpha_{\mathbf{k},1} - \alpha^{\dagger}_{\mathbf{k},2}\alpha_{\mathbf{k},2} \right) + + \varepsilon_{\mathbf{k},2} \left(\alpha^{\dagger}_{\mathbf{k},3}\alpha_{\mathbf{k},3} - \alpha^{\dagger}_{\mathbf{k},4}\alpha_{\mathbf{k},4} \right) \Big] \quad (5)$$

and the eigenvalues are:

$$\varepsilon_{\mathbf{k},1} = \sqrt{\frac{t_\perp^2}{2} + f^2 + |\gamma_{\mathbf{k}}|^2 + \sqrt{\frac{t_\perp^4}{4} + |\gamma_{\mathbf{k}}|^2(t_\perp^2 + 4f^2)}}$$

$$\varepsilon_{\mathbf{k},2} = \sqrt{\frac{t_\perp^2}{2} + f^2 + |\gamma_{\mathbf{k}}|^2 - \sqrt{\frac{t_\perp^4}{4} + |\gamma_{\mathbf{k}}|^2(t_\perp^2 + 4f^2)}}. \quad (6)$$

and thus represent the electronic dispersion law for the bi-layer graphene (see fig. 2).

Based on the demonstrated results, and schematically shown in fig. 2, an electric-bias increases the electronic band-gap; this behaviour shows that this material has a variable electronic gap dependant on the applied electric field.

3 Effect of Impurities

Based on the above demonstrated results, it is interested to study the impurity effects on the spectrum rearrangement for the bi-layer graphene system.

As observed on other semiconductors with relevant technological impact, impurity effects are decisive for the reliability of the electronic performance of the bi-layer graphene. Impurities and/or dopants are sometimes inevitable during the growth or the processing of the materials. Considerable effort has hence been directed toward the study of defects in semiconductors and insulators and how these can affect device properties and reliability. Much of the present-day engineering of materials consists of pragmatic strategies of trying to control defect densities by processing control and annealing. [17]

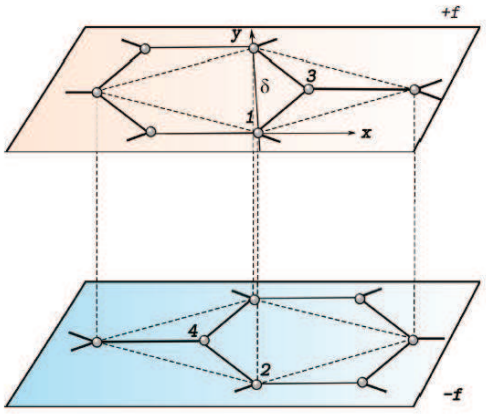

Figure 1. Bernal stacking for the structure of bi-layer graphene. The ±f potential results in the application of an electric field between two layers.

The uncontrolled presence of defects may cause unreliability, being the main source for electrical failure and breakdown of the material. Trapped charges in defects causes a shift in the gate threshold voltage of the transistor; it can also change with time, shifting the threshold voltage with time, thus leading to instability of operating characteristics. Also, trapped charge scatters carriers in the channel and lowers the carrier mobility. [17]

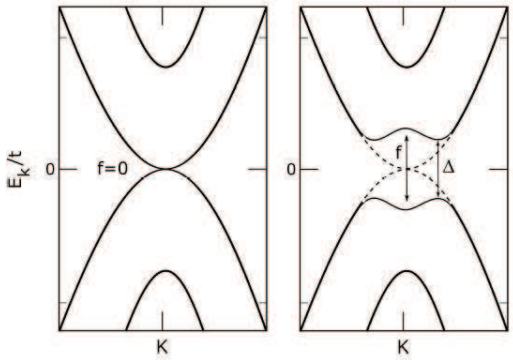

Figure 2. The band structure of bi-layer graphene. When there is no applied electric field, f = 0, the structure is a gapless semi-conductor, but when an electric field is applied, f ≠ 0, the system becomes insulator, and the width of the electronic gap Δ is controlled by the applied field f.

Among such defects are impurities, such as interstitial hydrogen, that can be unintentionally incorporated during the growth environment.[4] Source gases contain hydrogen as carrier gas and in molecular beam epitaxy hydrogen is the prevailing background impurity, exhibiting complex behaviours when introduced in materials. [4]

4 Density Functional Theory Calculations of Bi-layer Graphene

In density functional theory (DFT) [21] the electronic orbitals are solutions of a set of Schrödinger-like equations, referred to as Kohn-Sham equations, from which potential terms depend on the electron density. The Kohn-Sham method assumes that, for each interacting ground state density $n(\vec{r})$, there is a non-interacting electron system with the same ground state density. The interacting ground state is thus obtained through the solution of the Kohn-Sham equations that have the form of the single-particle Schrödinger equation

$$\Big[-\frac{\nabla^2}{2}+v_{\text{KS}}[n(\vec{r})]\Big]\varphi_i(\vec{r})=\epsilon_i\varphi_i(\vec{r}),$$

where v_{KS} is the Kohn-Sham potential, with a functional dependence on the electronic density, n, which is defined in terms of the Kohn-Sham wave-functions by $n(\vec{r}) = \sum_i^{occ}|\varphi_i(\vec{r})|^2$.

This potential can be defined as the sum of the external potential, which is the Coulomb attraction between the bare nucleus and the electrons, the Hartree term, representing the electrostatic energy of the electron in the field generated by the total density; and the exchange and correlation potential (xc), thus

$$v_{\text{KS}}[n(\vec{r})]=v_{\text{ext}}(\vec{r})+v_{\text{Hartree}}[n(\vec{r})]+v_{\text{xc}}[n(\vec{r})]. \quad (7)$$

The last term of eq. 7 is the exchange-correlation potential, that takes into account the many-body effects in the form of an exchange-correlation functional and is defined by the functional derivative of the xc energy

$$v_{\text{xc}}[n(\vec{r})]=\frac{\delta E_{\text{xc}}}{\delta n(\vec{r})}. \quad (8)$$

The only approximation in DFT is related to the non-trivial many-body effects, which can be grouped into one of the terms of the non-interacting Kohn-Sham potential - the exchange-correlation (xc) functional. This functional has to be obtained by approximations, developed for a wide variety of physical systems and applications.

The simplest approximation to represent an exchange-correlation potential is to apply the Local Density Approximation (LDA) or its spin-relaxed version, the Local Spin-Density Approximation (LSDA). Within this approximation the potential depends only on the value of the density at $\vec{r}$ [22]. The correlation functional is obtained by a simple parametrized form fitted to several densities calculated by using quantum Monte Carlo simulations of Ceperley and Alder [23] on homogeneous electron gases. The most common parametrizations in use are PZ81 [24], PW92 [25].

The generalized gradient approximation (GGA), another well known functional, differs from the LDA because this functional also incorporates the effects of inhomogeneities by including the gradient of the electron density, ∇n (semi-local method). In this case the most widely used parametrizations are the Perdew-Wang (PW91) [26] and the Perdew-Burke-Ernzerhof (PBE) [27].

Some results, obtained within the L(S)DA approximation are found to be in very good agreement with experimental data, such as equilibrium structures, harmonic stretch frequencies, and charge moments [28]. Although successful for some systems, this approach can fail, for example, by incorrectly predicting negative ions to be unstable, underestimating the fundamental energy gaps of semiconductors and insulators, overestimating the length of hydrogen bonds. Similar to the LDA, GGA also fails to describe energy band-gaps, which are a crucial physical quantity if one intends to study, e.g. the impurity levels in doped semiconductors. Another common deficiency of (semi-)local approximations is their incorrect description of long-range correlation, mainly the van-der-Waals (vdW) interactions. Inspite these failures, these functionals provide reasonable accuracy for forces, charge-densities, energy barriers, and are computationally inexpensive to obtain the ground-state properties of periodic systems.

Improved exchange-correlation functionals have been formulated since then, and are grouped into five *rungs* in a sequence of chemical accuracy, known as *the Jacob's ladder of density functional approximations* [29]. As the ladder is ascended, the functionals incorporate higher levels of theory with increasingly complex parameters.

In order to obtain a *ab-initio* band-structure of bi-layer graphene, as a function of different applied electric-bias, and compare to the tight-binding approximation, DFT calculations were performed, as implemented in the Quantum-Espresso code package [30]. The semi-local generalized-gradient approximation functional with the PBE parametrization [27] was employed for electronic-structure the calculations. Projector augmented-wave (PAW) [33, 32, 31] pseudopotentials were used to represent the effective-potential of the system.

The starting point for the present calculations, was a full structural relaxation for the unit-cell of the AB stacking of bi-layer graphene, performed with a plane-wave cut-off of 900 eV. Such a high cut-off was found necessary to converge the total energy of the system. In order to sample the Brillouin zone (BZ) a Γ-centred Monkhorst-Pack mesh [34] of $44\times44\times1$ was employed. Since (semi-)local DFT functionals do not take into account van der Waals interactions, which are essential for many covalent bonded systems and systems dominated by dispersion forces, i.e. interlayer bonding of bi-layer graphene, dispersion effects were included via semiempirical atom pairwise interactions using the DFT-D2 methods by Grimme *et al* [35].

In Fig. 1 the electronic band structure is represented for the system, where one may observe that at 0 eV, the valence-band maximum and conduction-band minimum are joint together, thus exhibiting a zero band-gap at the

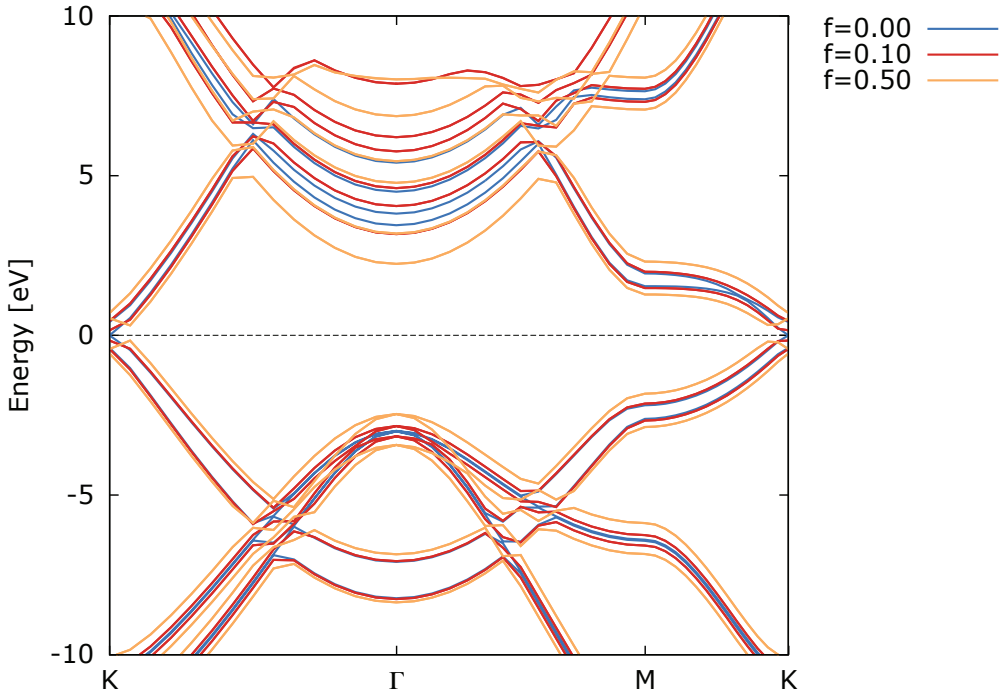

Figure 1: Electronic band-structure of bi-layer graphene for the AB-stacking system, for different applied electric-bias. The units of the electric-bias is given by eV/A.

high-symmetry point K. By applying an electric-bias, the gap starts to open. The width of the gap increases with increasing bias, evidencing a tunable electronic band-gap, similar to what was experimentally observed [36], and similar to results obtained through the tight-binding method.

References

[1] Y. Araki. Chiral Symmetry Restoration in Monolayer Graphene Induced by Kekule Distortion. *Phys. Rev. B*, 84:113402, 2011.

[2] Y. Araki and T. Hatsuda. Chiral Gap and Collective excitations in Monolayer Graphene from Strong Coupling Expansion of Lattice Gauge Theory. *Phys. Rev. B*, 82:121403(R), 2010.

[3] C. Berger, Z. Song, T. Li, X. Li, A. Y. Ogbazghi, R. Feng, Z. Dai, A. N. Marchenkov, E. H. Conrad, P. N. First, and W. A. de Heer. Ultrathin Epitaxial Graphite: 2D Electron Gas Properties and a Route Toward Graphene-Based Nanoelectronics. *J. Phys. Chem.*, 108:19912, 2004.

[4] C. G. Van de Walle and J. Neugebauer. Universal Alignment of Hydrogen Levels in Semiconductors, Insulators and Solutions. *Nature (London)*, 423:626, 2003.

[5] E. V. Gorbar, V. P. Gusynin, V. A. Miransky, and I. A. Shovkovy. Magnetic Field Driven Metal-Insulator Phase Transition in Planar Systems. *Phys. Rev. B*, 66:045108, 2002.

[6] V. P. Gusynin, V. A. Miransky, and I. A. Shovkovy. Catalysis of Dynamical Flavor Symmetry Breaking by a Magnetic Field in 2 + 1 Dimensions. *Phys. Rev. Lett.*, 73:3499, 1994.

[7] V. P. Gusynin and S. G. Sharapov. Unconventional Integer Quantum Hall Effect in Graphene. *Phys. Rev. Lett.*, 95:146801, 2005.

[8] D. V. Khveschenko, A. G. Yashenkin, and I. V. Gornyj. Interacting Random Dirac Fermions in Superconducting Cuprates. *Phys. Rev. Lett.*, 86:4668, 2001.

[9] D. V. Khveshchenko. Ghost Excitonic Insulator Transition in Layered Graphite. *Phys. Rev. Lett.*, 87:246802, 2001.

[10] D. V. Khveshchenko. Magnetic-Field-Induced Insulating Behavior in Highly Oriented Pyrolitic Graphite. *Phys. Rev. Lett.*, 87:206401, 2001.

[11] D. V. Khveshchenko. Electron Localization Properties in Graphene. *Phys. Rev. Lett.*, 97:036802, 2006.

[12] Y. Kopelevich, P. Esquinazi, J. H. S. Torres, and S. Moehlecke. *J. Low Temp. Phys.*, 119:691, 2000.

[13] K. S. Novoselov, A. K. Geim, S. V. Morozov, D. Jaing, M. I. Katsnelson, I. V. Grigorieva, S. V. Dubonos, and A. A. Firsov. Two-Dimensional Gas of Massless Dirac Fermions in Graphene. *Nature*, 438:197, 2005.

[14] K. S. Novoselov, A. K. Geim, S. V. Morozov, D. Jaing, Y. Zhang, S. V. Dubonos, I. V. Grigorieva, and A. A. Firsov. Electric Field Effect in Atomically Thin Carbon Films. *Science*, 306:666, 2004.

[15] K. S. Novoselov, E. McCann, S. V. Morozov, V. I. Fal'ko, M. I. Katsnelson, U. Zeitler, D. Jiang, F. Schedin, and A. K. Geim. Unconventional Quantum Hall Effect and Berry's Phase of 2π in Bilayer Graphene. *Nature Physics*, 2:177, 2006.

[16] N. M. R. Peres, F. Guinea, and A. H. Castro Neto. Electronic Properties of Two-Dimensional Carbon. *Annals of Physics*, 321:1559, 2006.

[17] J. Robertson. High Dielectric Constant Gate Oxides for Metal Oxide Si Transistors. *Rep. Prog. Phys.*, 69:332, 2006.

[18] G. Semenoff. Condensed-Matter Simulation of a Three-Dimensional Anomaly. *Phys. Rev. Lett.*, 53:2449, 1984.

[19] P. R. Wallace. The Band Theory of Graphite. *Phys. Rev.*, 77:622, 1947.

[20] Y.-Y. Zhang, C. Fang, X. Zhou, K. Seo, W.-F. Tsai, B. A. Bernevig, and J. Hu. Quasiparticle Scattering Interference in Superconducting Iron Pnictides. *Phys. Rev. B*, 80:094528, 2009.

[21] W. Kohn and L. Sham, Phys. Rev. 140, A1133, 1965. P. Hohenberg and W. Kohn, Phys. Rev. 136, B864, 1964.

[22] F. Nogueira, A. Castro, and M. A. L. Marques. A Primer in Density Functional Theory, chapter 6, pages 218. Springer, 2002.

[23] D. M. Ceperley and B. J. Alder, Phys. Rev. Lett. 45, 566, 1980.

[24] J. P. Perdew and A. Zunger, Phys. Rev. B 23, 5048, 1981.

[25] J. P. Perdew and Y. Wang, Phys. Rev. B 45, 13244, 1992.

[26] J. P. Perdew, J. A. Chevary, S. H. Vosko, K. A. Jackson, M. R. Pederson, D. J. Singh, and C. Fiolhais, Phys. Rev. B 46, 6671, 1992. J. P. Perdew, J. A. Chevary, S. H. Vosko, K. A. Jackson, M. R. Pederson, D. J. Singh, and C. Fiolhais, Phys. Rev. B 48, 4978E, 1993.

[27] J. P. Perdew, K. Burke, and M. Ernzerhof, Phys.l Rev. Lett. 77, 3865, 1996. J. P. Perdew, K. Burke, and M. Ernzerhof, Phys. Rev. Lett. 78, 1396(E), 1997.

[28] W. Koch and M. C. Holthausen. A Chemist's Guide to Density Functional Theory. Wiley-VCH Verlag GmbH, second edition edition, 2001.

[29] J. P. Perdew and S. Kurth. A Primer in Density Functional Theory, chapter 1, page 1. Springer, 2002.

[30] P. Giannozzi, S. Baroni N. Bonini, M. Calandra, R. Car, C. Cavazzoni, D. Ceresoli, Guido. L. Chiarotti, M. Cococcioni, I. Dabo, A. Dal Corso, S. de Gironcoli, S. Fabris, G. Fratesi, R. Gebauer, U. Gerstmann, C. Gougoussis, A. Kokalj, M. Lazzeri, L. Martin-Samos, N. Marzari, F. Mauri, R. Mazzarello, S. Paolini, A. Pasquarello, L. Paulatto, C. Sbraccia, S. Scandolo, G. Sclauzero, A. P. Seitsonen, A. Smogunov, P. Umari and R. M. Wentzcovitch, J.Phys.:Condens.Matter 21, 395502, 2009.

[31] P. E. Blöchl. Projector Augmented-Wave Method. Phys. Rev. B, 50:17953, 1994.

[32] G. Kresse and D. Joubert, Phys. Rev. B 59, 1758, 1999.

[33] $\mathrm{C.pbe-n-kjpaw\_psl.0.1.UPF}$ pseudopotential was downloaded from http://www.quantum-espresso.org.

[34] H. J. Monkhorst and J. D. Pack. Special points for brillouin-zone integrations. Phyiscal Review B, 13:5188, 1976.

[35] S. Grimme, J. Comp. Chem. 27, 1787 (2006).

[36] Y. Zhang, T.-T. Tang, C. Girit, Z. Hao, M. C. Martin, A. Zettl, M. F. Crommie, Y. R. Shen and F. Wang, Nature 459, 820, 2009.